

## Expression of the DNA Repair Enzyme, Photolyase, in Developmental Tissues and Larvae, and in Response to Ambient UV-R in the Antarctic Sea Urchin *Sterechinus neumayeri*

Nikolas Isely<sup>1,2</sup>, Miles Lamare<sup>\*1</sup>, Craig Marshall<sup>2</sup> and Mike Barker<sup>2</sup>

<sup>1</sup>Department of Marine Science, University of Otago, Dunedin, New Zealand

<sup>2</sup>Genetics Otago and Department of Biochemistry, University of Otago, Dunedin, New Zealand

Received 9 December 2008, accepted 23 February 2009, DOI: 10.1111/j.1751-1097.2009.00566.x

### ABSTRACT

Gene expression of the DNA repair enzyme, photolyase (E.C. 4.1.99.3) was examined in the gonads, eggs, embryos and larval stages of the Antarctic sea urchin, *Sterechinus neumayeri*. Partial sequencing of the gene revealed two highly conserved regions, including a 300 bp region representing the binding site for the cofactor flavin adenine dinucleotide. The second 1200 bp region, likely representing a second light-harvesting cofactor binding site, was identified in a second sea urchin species, *Strongylocentrotus frascicanus*. Probes for photolyase were developed from the shorter sequence, and expression in sea urchin developmental tissue and stages, and in response to *in situ* exposure to ultraviolet radiation was quantified using PCR and RT-qPCR, with concentrations of photolyase normalized to actin concentrations. Photolyase was expressed in all tissues and developmental stages examined. In controlled field-based experiments in McMurdo Sound, Antarctica, we found evidence of both constitutive expression of photolyase and induction in response to *in situ* exposure of embryos to UV-R. Induction of photolyase was observed in response to greater ambient UV-R (such as shallower water depths or sea ice-free regions).

### INTRODUCTION

Stratospheric ozone depletion over the Antarctic in the austral spring (the *Ozone hole*) elevates UV-B radiation (290–315 nm). Previous research has shown that UV-B has a deleterious effect on a range of Antarctic organisms including bacteria (1), phytoplankton (2), and a suite of zooplankton species (3,4), and increases in UV-R will have significant effects on organisms in this area (5). Effects observed to date include photoinhibition (2), reduced survival and developmental abnormalities (3–5), increased oxidative stress and DNA damage (4,6,7). The overall effect of ozone depletion on organisms is however, equivocal, with some studies identifying greater UV-B effects during ozone depletion (2,3) while others have found only limited effects of ozone depletion (8,9).

Ultraviolet radiation causes damage to DNA across its spectral range, with the shorter UV-B (280–320 nm) wavelengths causing direct damage in the form of DNA lesions,

while longer wavelength UV-A (320–400 nm) causes both direct and indirect damage *via* oxidation of DNA (most commonly 8-oxo-7,8-dihydro-2'-deoxyguanosine), strand breaks and DNA crosslinks (10,11). The dominant forms of DNA damage are cyclobutane pyrimidine dimers (CPDs), the result of UV-R-induced dimerization of adjacent pyrimidine nucleotide bases (cytosine and thymine) to form either the predominant ( $\approx 85\%$ ) CPD or to a lesser extent ( $\approx 15\%$ ), 6-4 photoproducts (6-4PP).

The two principal mechanisms of removing DNA dimers are nucleotide excision repair (NER) and photoreaction. NER does not directly reverse the formation of DNA dimers, but uses a suite of enzymes (primarily glycosylases and endonucleases) to detect, remove and replace DNA lesions with undamaged DNA nucleotides (10). NER is highly conserved and present in most organisms, although the mechanism involves a greater suite of enzymes in eukaryotes compared with prokaryotes (10). The second mechanism of DNA repair is photoreaction, a light-dependent reaction mediated by photolyase enzymes (EC 4.1.99.3) that utilize the energy in light of wavelengths between 320 and 500 nm to directly resolve CPD into the constituent nucleotides in a largely error-free reaction (12). Photolyase is a monomeric enzyme of 420–616 amino acids, containing a catalytic cofactor, flavin adenine dinucleotide (FAD) and typically a light-harvesting cofactor, of which three have been identified to date (5,10-methyltetrahydrofolate, 8-hydroxy-5-deaza-riboflavin and flavin mononucleotide) (13–16). Photoreactivation of CPDs by photolyase is a UV-A or blue light-driven process, where a photon is initially captured by the light-harvesting cofactor and transferred to FAD. Subsequently, an electron is indirectly passed (*via* an alanine residue) to the CPD dimer, thereby restoring the DNA to a normal configuration. Once the DNA dimer is split, the electron is transferred back to FADH<sup>-</sup> (17). Photolyase is widely distributed in eukaryotes, eubacteria and archaea and is consequently thought to be very ancient (15). Similarity among photolyase sequences ranges from about 15% to 70%. The region showing the greatest amount of conservation is the 150 amino acids at the C-terminus that contains the FAD binding site (12,18).

Recent findings indicate that Antarctic species may be more susceptible to the effects of UV-B, than their more temperate counterparts. For example, embryos of Antarctic sea urchins accumulated significantly more DNA lesions (CPDs) after

\*Corresponding author email: miles.lamare@otago.ac.nz (Miles Lamare)

© 2009 The Authors. Journal Compilation. The American Society of Photobiology 0031-8655/09

exposure to ambient UV-R when compared with temperate and tropical species (6). There are a number of possible causes of such DNA damage, including a lower sunscreen capacity and a reduced ability to repair damaged DNA in Antarctic embryos. Reduced DNA repair may be important in sea urchin embryos, as those from the Antarctic sea urchin, *Sterechinus neumayeri*, show significantly slower rates of DNA photoreactivation than do their temperate and tropical counterparts (19).

We investigated the expression of the DNA photoreactivation enzyme photolyase, in the Antarctic sea urchin *S. neumayeri* after exposure to ambient ultraviolet radiation. The initial aim of this research was to sequence the photolyase gene and examine its expression in *S. neumayeri*. Prior to this study, few molecular investigations had been carried out on photolyase in higher animals, none of which involved marine invertebrates. Information available on photolyase in sea urchins is also limited, and even in the recently completed sequence of the *Strongylocentrotus purpuratus* genome, much of the sequence information remains unannotated. We used a partial sequence predicted to be CPD photolyase for *S. purpuratus* and for *Gallus gallus* photolyase to design PCR primers to amplify a region of cDNA corresponding to photolyase in four sea urchin species (*Strongylocentrotus franciscanus*, *S. purpuratus*, *Evechinus chloroticus* and *S. neumayeri*), including an almost complete photolyase sequence for the sea urchin *S. franciscanus*. Once obtained, the information contained in the new sequences was used to design gene-specific primers for measuring photolyase expression by RT-qPCR. Using RT-qPCR, we focus our investigations on photolyase expression in *S. neumayeri* embryos in response to ambient UV-R exposure.

*Sterechinus neumayeri* is endemic to the shallow coastal waters of the Antarctic. The species has a relatively long-lived, planktotrophic larva that inhabits surface waters for up to 4 months during the spring and early summer (20). The larvae have relatively slow metabolic rates in comparison with temperate and tropical echinoid larvae (21). Given that *S. neumayeri* is susceptible to UV-R in its natural environment (3,5,8), understanding the response of *S. neumayeri* embryos to UV-R exposure in terms of photolyase expression will give us further insight into the potential effects of future climate change (*i.e.* increased UV-R exposure as a result of ozone depletion and future reduced sea ice coverage) at the molecular level.

## MATERIALS AND METHODS

**Sea urchin tissue collection and RNA isolation.** Samples of gonad tissue, embryos and larvae were obtained from three echinoids: *Strongylocentrotus franciscanus* (Family: Strongylocentrotidae) collected from California; *Evechinus chloroticus* Valenciennes (Family: Echinometridae) collected from southern New Zealand; and *S. neumayeri* Meissner (Family: Echinidae) collected from McMurdo Sound, Antarctica. Samples were preserved by flash freezing in either liquid nitrogen or dry ice, or preservation in RNAlater (Ambion) and temporarily stored at  $-20^{\circ}\text{C}$ . Gonad samples stored in RNAlater were shown to contain intact RNA for up to 4 days after collection. For long-term storage all samples were kept at  $-80^{\circ}\text{C}$ . RNA was extracted using a method based on the single-step technique of Chomczynski and Sacchi (22). Total RNA was isolated using Trizol Reagent (Invitrogen) according to the manufacturer's protocol, although all volumes used were 1/10th of that recommended in the original protocol. RNA concentration and

purity were quantified using a NanoDrop spectrophotometer (NanoDrop), while RNA quality was checked by analyzing samples on a 1% formaldehyde agarose gel containing ethidium bromide.

**Library screen.** Oligonucleotides in this study were synthesized by either Integrated DNA Technologies or Invitrogen. Primers were designed by Primer3 (18) or by hand against an alignment of two sequences. *Photolyase*: forward 5'-CAC AGG TTG TAC TTC TTG TAC CGG TTG-3'; reverse 5'-GGT TCG TGA GGG TAA GAT GCA TGG-3'. *Actin*: forward 5'-AAG GAC AGC TAC GTC GGA GA-3'; reverse 5'-GCA ACA CGG AGT TCG TTG TA-3'. Primers were re-suspended in nuclease free water (Ambion) to make a stock solution with a concentration of 0.0382 M. Aliquots from the stock solution were then diluted to a concentration of 10  $\mu\text{M}$  for use in PCR. Reverse transcription was made using a Super Script III kit (Invitrogen), and PCR products were purified using the MinElute PCR Purification Kit (Qiagen) with concentrations determined using a NanoDrop (NanoDrop) spectrophotometer. The purified PCR product was cloned into the pGEM-T Easy Vector System 1 (Promega) and the recombinant plasmid transformed into *Escherichia coli* JM109 High Efficiency Competent Cells (Promega) and plated on LB agar medium containing ampicillin. Colonies containing the inserted PCR product were selected by a color screen and then grown overnight in 10 mL of LB medium with ampicillin. Plasmid DNA was prepared using the PureLink Quick Plasmid Miniprep Kit (Invitrogen). Sequencing of plasmid DNA was made by the Allan Wilson Center Genome Services at Massey University (NZ), and the sequence of interest BLASTed against databases at the National Center for Biotechnology Information (NCBI).

**Reverse transcriptase-polymerase chain reaction (RT-PCR).** Genomic DNA was removed from RNA samples prior to reverse transcription by treatment with amplification grade DNase I (Invitrogen). Reverse transcription was made using a Transcriptor First Strand cDNA Synthesis Kit (Roche, Germany), with the amount of RNA used in the reaction varying depending upon the experiment. RT-QPCR was carried out using the LightCycler 480 (Roche) and LightCycler 480 SYBR Green 1 Master (Roche) reagent kit, or the LightCycler 2.0 system (Roche) and LightCycler FastStart DNA Master<sup>PLUS</sup> SYBR Green 1 (Roche) reagent kit. Reactions were carried out according to the manufacturer's protocol with one modification; reaction volumes of 10  $\mu\text{L}$  were used instead of 20  $\mu\text{L}$ . The template added to each reaction was a 1/20 dilution of the cDNA.

**Standard curve.** For quantifying the concentration of cDNA for a particular transcript, standard curves were constructed for each set of primers to calculate both amplification efficiency and error. Curves were constructed using RNA isolated from *S. neumayeri* larvae that had been frozen 2 h after being exposed to direct UV light for 1 h. This sample was chosen because of its high concentration of RNA (2259.8 ng  $\mu\text{L}^{-1}$ ). RNA was treated with amplification grade DNase I (Invitrogen). The standard curves were constructed by analyzing duplicate samples of diluted cDNA at the following dilutions: 1/20, 1/100, 1/200, 1/500, 1/1000, 1/2000 and 1/5000.

**RT-QPCR product analysis.** RT-QPCR products were analyzed by both melt curves and gel electrophoresis. Melt curves were used to ensure only one product was formed during QPCR amplification and were calculated automatically by the LightCycler 4.0 Software (Roche). PCR products were analyzed for size using gel electrophoresis.

**RT-QPCR reaction setup. Lightcycler 2.0.** Reaction volumes of 10  $\mu\text{L}$  were used for all reactions and were set up in 20  $\mu\text{L}$  capillary tubes (Roche). All reactions were set up according to the manufacturer's protocol using the LightCycler FastStart DNA Master<sup>PLUS</sup> SYBR Green 1 kit (Roche). The template added to each reaction was a 1/20 dilution of the cDNA. DNA amplification conditions were as follows: 5 min at 95°C (denaturation step); 50 cycles of 5 s at 95°C, 5 s at 58°C, 4.4 s at 72°C; 30 s at 95°C; 65°C to 95°C at a rate of 2.2°C  $\text{s}^{-1}$  (melting curve analysis).

**Lightcycler 480.** Reaction volumes of 10  $\mu\text{L}$  were used for all reactions and were set up in 96 well plates (Roche). Actin reactions were composed of the following constituents added in the order listed: 5  $\mu\text{L}$  LightCycler 480 SYBR Green 1 Master (Roche), 0.5  $\mu\text{L}$  of each primer from a stock solution of 10  $\mu\text{M}$ , 1.0  $\mu\text{L}$  H<sub>2</sub>O and 3  $\mu\text{L}$  of

template that had been diluted to a 1/20 concentration. Photolyase reactions were similar but contained 0.25  $\mu\text{L}$  of each primer and 1.5  $\mu\text{L}$  of  $\text{H}_2\text{O}$ .

**Statistical analysis and interpretation of RT-QPCR data.** Absolute quantification of templates was made using LightCycler 4.0 Software (Roche). This was accomplished by construction of a standard curve for each primer set with samples of a known concentration. The standard curve was constructed by plotting the log of the concentration of the standards against their crossing point values. The crossing points of unknown samples were then used to calculate their concentration from the standard curve. Photolyase was normalized by dividing its concentration by that of actin in the same sample. Replicates were averaged, and the standard error of the mean was calculated using GraphPad InStat (GraphPad).

**Field exposures.** *Sterechninus* gametes were obtained by induced spawning of ripe individuals using an inter-coelomic injection of 0.5 M KCl, and fertilization of eggs was achieved by adding several drops of dilute sperm. The fertilization rate was determined from the appearance of a fertilization envelope, and only batches of eggs with a fertilization rate >95% were used in experiments. Fertilized eggs were washed by serial partial water changes prior to experimentation.

**In situ exposures of embryos to ambient solar radiation** were undertaken by out-planting bagged embryos onto experimental PVC racks (31 cm  $\times$  26 cm horizontal dimensions) located at various depths on a moored rope (3). The depths of the racks were 1, 2, 5 and 10 m below the sea surface or sea ice surface. At each depth, embryos were subjected to one of two light treatments: (1) photosynthetically active radiation (PAR) but no UV-R and (2) PAR + UVA + UVB. The two treatments were achieved using Plexiglas filters (170 mm  $\times$  170 mm) with different transmission rates of UV-B, UV-A and PAR. Transmission of UV-R and visible light by the filters is reported in Lamare *et al.* (6).

For out-planting, embryos were bagged in 125 mL whirl-pack bags that are transparent to both UV-R and visible light. The embryos in the bags were at a density of 5–10  $\text{mL}^{-1}$ . For each treatment at each depth, three replicate bags of embryo were used, giving a total of 27 bags per experiment. *In situ* exposures were made at Cape Evans (77°38.10'S, 166°25.00'E) from 31 October to 7 November 2007. At Cape Evans, experiments were placed under a 2 m sea ice canopy that had formed during the 2007 winter. A further set of *in situ* exposures was made at the sea ice edge (77°37.643'S, 165°39.588'E) from 1 to 10 November 2007. The sea ice coverage at the ice edge was  $\approx$ 5 to 20 cm thick and was likely less than 1 week old. At the end of each experiment the bags were removed from the racks and immediately placed into a dark thermally insulated container filled with ambient temperature seawater. The samples were then processed as soon as possible (and within 9 h of collection). Processing was made under dim yellow lights to minimize postexposure photodamage or photoreactivation in the embryos. For RNA isolation 60 larvae were counted and placed in a clean RNase-free 1.5 mL microfuge tube, and flash frozen in liquid nitrogen.

**Environmental ultraviolet radiation measurements.** Spectral irradiances were measured using a LiCor Li1800UW submersible spectroradiometer that was factory calibrated in May 2005 using National Institute of Standards and Technology traceable standards. During the times of *in situ* embryo experiments, spectral irradiance was measured at the surface and at 0.5, 1.0, 2.0, 5.0, 10 and 20.0 m depth. Scans of spectral irradiance ( $\text{W m}^{-2} \text{nm}^{-1}$ ) were made between 300 and 750 nm at 2 nm intervals, with three consecutive replicate scans made for each depth (replicates averaged). All scans were made between 1200 and 1400 h, and when the sky was cloudless.

Optical properties of the water column were quantified by calculation of bulk spectral attenuation coefficients ( $K_d \text{m}^{-1}$ ) at each wavelength using the equation:

$$I_D(\lambda) = I_0(\lambda)e^{-kd} \quad (1)$$

where  $I_D(\lambda)$  is the irradiance at wavelength ( $\lambda$ ) at depth  $d$ ,  $I_0(\lambda)$  is the irradiance at wavelength ( $\lambda$ ) at the surface and  $k$  is the light extinction coefficient. For each scan, UV-B (300–320 nm,  $\text{W m}^{-2}$ ), UV-A (320–400 nm,  $\text{W m}^{-2}$ ) and PAR (400–750 nm,  $\mu\text{mol quanta m}^{-2} \text{s}^{-1}$ ) were also calculated. The attenuation of UV-B, UV-A and PAR was then calculated using Eq. 1. Ambient UV-B, UV-A and PAR (400–600 nm), as well as a spectral irradiance (290–400 nm) over the *in situ* exposure

periods were obtained from data collected by the National Science Foundation UVR Monitoring Program using a SUV-100 spectroradiometer (Biospherical Instruments, San Diego). Surface spectral measurements were converted to spectral irradiances at our experimental depths (0.5, 1.5 and 4 or 5 m) using our bulk spectral attenuation coefficients ( $K_d \text{m}^{-1}$ ) measured for each wavelength Eq. (1).

**Statistics.** Two-way analysis of variance tested for the effects of depth and light treatment on photolyase expression ([mRNA] normalized to actin) for Cape Evans (31 October to 7 November 2007) from four depths. Three-way analyses of variance tested for the effects of site, depth and light treatment on photolyase expression ([mRNA] normalized to actin) for Cape Evans (31 October to 7 November 2007) and the sea ice edge (1 November to 10 November 2007). Normalized photolyase concentrations were tested for equal variance using Levene's test. If the variance was not equal the data was  $\ln(x + 1)$  transformed. Statistical tests were run using JMP7.0 software (SAS Institute Inc.).

## RESULTS

### Photolyase sequences

A 300 bp sequence was amplified in the sea urchins *S. neumayeri* (Family Echinidae), *S. franciscanus* (Family Strongylocentrotidae) and *E. chloroticus* (Family Echinometridae) (Fig. 1). This sequence had a high degree of homology with photolyase of *S. purpuratus* (Family Strongylocentrotidae) and *Gallus gallus*. The  $e$  values of the sequences for *S. neumayeri*, *E. chloroticus* and *S. franciscanus* when aligned to *S. purpuratus* were very small ( $1.9107 \times 10^{-101}$ ). When compared with *G. gallus* the  $e$  values are not as low, but still of significance ( $1.759 \times 10^{-21}$ ).

### Photolyase expression in the embryonic tissue developmental stages

Photolyase mRNA was present in detectable levels in the gonad of *S. franciscanus*, and the gonad, fertilized eggs, blastula, prism and pluteus stage larvae of *E. chloroticus* and *S. neumayeri* (Fig. 2). As the analysis was made using a nonquantitative PCR, the relative levels of mRNA in each tissue were not established.

### Irradiances

**Surface irradiances.** Maximum ambient UV-B (290–320 nm), UV-A and Vis light (400–600 nm) in McMurdo Sound were 1.92, 35.91 and 215  $\text{W m}^{-2}$ , respectively, in the period between 31 October and 10 November 2007. During this time, UV-B and UV-A irradiances averaged 0.54 and 12.93  $\text{W m}^{-2}$ , respectively (Fig. 3), and average daily doses of UV-B of 43  $\text{kJ m}^{-2} \text{day}^{-1}$  and UV-A of 1037  $\text{kJ m}^{-2} \text{day}^{-1}$ . The average atmospheric ozone concentration was 218 DU and the range was from 167.9 to 311.5 DU over the 11-day period (Fig. 3). The UVB:Vis ratio ranged from 0.0001 to 0.016, and was greatest during the low ozone concentrations that occurred between 3 and 10 November (Fig. 3).

**Underwater irradiances.** Penetration of UV-B and UV-A through the sea ice and underlying water column was greater at the sea ice edge compared with Cape Evans (Fig. 4). At Cape Evans, measured UV-B irradiances at 0.5, 5 and 10 m depth were 0.023, 0.012 and 0.003  $\text{W m}^{-2} \text{s}^{-1}$ , respectively, while irradiances at equivalent depths at the sea ice edge were 0.51,

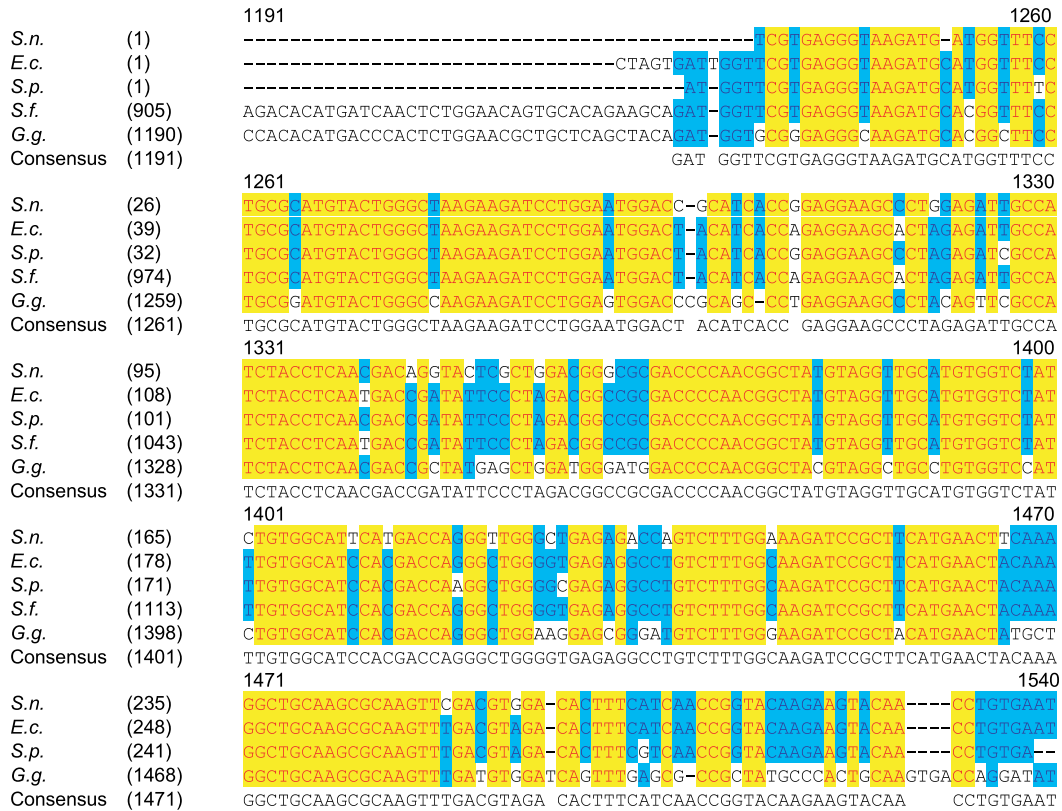


**Figure 1.** Partial photolyase sequences for four species of sea urchin *Sterechinus neumayeri* (*S.n.*), *Evechinus chloroticus* (*E.c.*), *Strongylocentrotus franciscanus* (*S.f.*) and *Strongylocentrotus purpuratus* (*S.p.*) aligned with *Gallus gallus* (*G.g.*). The primers used to amplify these sequences were Photolyase Forward and Photolyase Reverse. The accession reference numbers for the *S. purpuratus* and *G. gallus* sequences are XM\_0011953181 and XM\_422729, respectively. Sequences were aligned in Vector NTI (Invitrogen). NCBI accession reference numbers for *S. neumayeri*, *E. chloroticus* and *S. franciscanus* are FJ812412, FJ812410 and FJ812411, respectively.

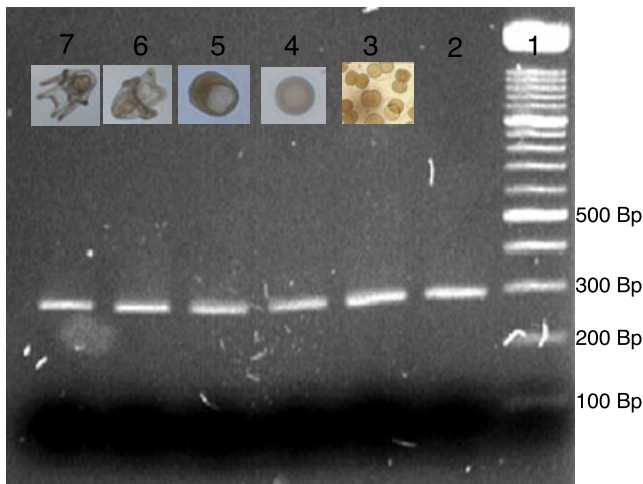


**Figure 2.** Agarose gel electrophoresis of the 300 bp photolyase PCR product. Bands indicate the presence (but not relative levels) of photolyase mRNA in the gonad tissue of adult gonad and various larval stages of the sea urchin *Sterechinus neumayeri*. Lane 1: 100 bp molecular weight ladder (Roche); Lane 2: gonad; Lane 3: fertilized eggs; Lane 4: blastula stage larvae; Lane 5: prism stage larvae; Lane 6: four-armed pluteus larvae; Lane 7: six-armed pluteus larvae. Images for each embryo and larval stage are given. A 2% agarose gel was run for 40 min at 140 V and visualized using ethidium bromide as described under Materials and Methods.

0.103 and 0.02 W m<sup>-2</sup> s<sup>-1</sup>, respectively (Fig. 4). UV-A and Vis irradiances were also higher at the sea ice edge (Fig. 4). The lower irradiances at Cape Evans can be attributed to the rapid attenuation of light by the sea ice, which resulted in a 96–97% decrease in UV-B, UV-A and Vis light (Fig. 4). In contrast, the attenuation of light by the sea ice at the ice edge only reduced UV-B by 32.9%, UV-A by 29.3% and Vis light by 34.6% (Fig. 4). The attenuation of light by the water column was lower at Cape Evans than at the sea ice edge (Fig. 4).

Spectral irradiances at the sea ice surface and through the water column at each site (Fig. 4) reflect the greater penetration of light at the sea ice edge. Wavelength specific attenuation highlights the rapid attenuation of light by the sea ice at Cape Evans, with  $K_d$  m<sup>-1</sup> approximately two- to three-fold greater compared with the sea ice at the ice edge (Fig. 5). Attenuation coefficients of the water column were very low at both sites (Fig. 5); the attenuation coefficient of light at 450 nm was 0.028 m<sup>-1</sup> at Cape Evans and 0.15 m<sup>-1</sup> at the sea ice edge. At both sites, the attenuation of light was greatest in the longer wavelengths (> 600 nm) and lowest in the blue (450–500 nm) and UV-R wavelengths (Fig. 5). Using both attenuation rates calculated from our spectral measurements with depth (Fig. 5) and continuous surface irradiances (Fig. 3), we estimated daily UV-R doses at our experimental depths over the periods of embryo exposures (Table 1). Total UV-R doses ranged from 1266 kJ m<sup>-2</sup> day<sup>-1</sup> at the sea ice

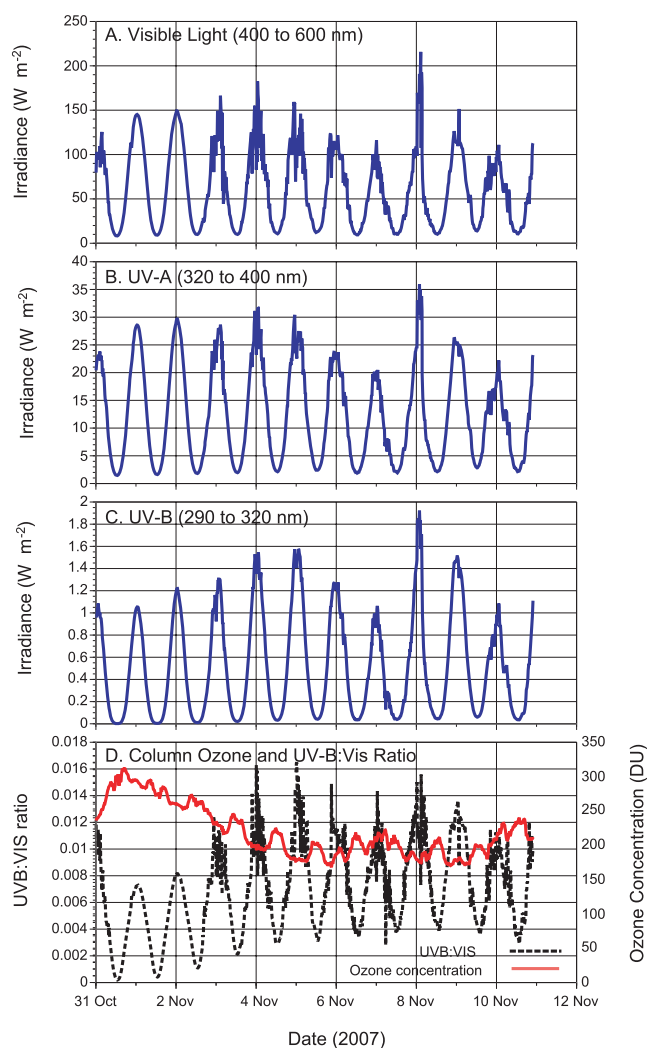


**Figure 3.** Ambient UV-B (290–320 nm), UV-A (320–400 nm) and PAR (400–600 nm) irradiances ( $\text{W m}^{-2}$ ), column ozone concentrations (DU) and UVB:Vis light at McMurdo Sound during the period of *in situ* embryo exposures (31 October to 10 November 2007).

edge 0.5 m depth to  $23.7 \text{ kJ m}^{-2} \text{ day}^{-1}$  at 10 m depth for Cape Evans.

#### *In situ* photolyase expression

Expression of photolyase in the blastula stage of *Strechinus* in the water column at Cape Evans between 31 and 7 November (Fig. 6) varied seven-fold depending on treatment and depth. Expression in the UV-T treatment increased with increasing daily UV-R dose, particularly at the shallowest depth (0.5 m) where a relative mRNA concentration of  $3.5 \times 10^{-3}$  corresponded with a  $105.4 \text{ kJ day}^{-1}$  UV-R dose. At the three deeper depths (1, 5 and 10 m), UV-R dose and mRNA concentration were positively related, although the magnitude of the dose variation ( $23.7\text{--}82.7 \text{ kJ day}^{-1}$ ) did not correspond to a similar range in mRNA concentrations ( $[\text{mRNA}] = 0.417\text{--}0.776 \times 10^{-3}$ ). Expression of mRNA in the UV-O treatments also increased with increasing UV-R dose, and was lower than the UV-T treatments in three of the four experimental depths. ANOVA indicated a significant effect of UV-R treatment

( $P = 0.051$ ) and depth ( $P = 0.0023$ ) (Table 2), with the difference mainly attributed to the significantly higher expression in the UV-T treatment at 0.5 m (Fig. 6).

Expression of photolyase in the blastula stage of *Strechinus* at Cape Evans and the sea ice edge during the second experimental period (31 October to 10 November 2007) (Fig. 7) varied eight-fold. Lowest mRNA concentrations were found in the Cape Evans samples and in the sea ice edge UV-O treatments ( $[\text{mRNA}] = 0.24\text{--}0.6 \times 10^{-3}$ ). Messenger RNA concentrations in the sea ice edge UV-T treatments were greater, especially in the shallow UV-T treatment ( $[\text{mRNA}] = 3.7 \times 10^{-3}$ ). ANOVA indicated that there was no significant difference in mRNA concentrations amongst UV-R treatments ( $P = 0.153$ ), depth ( $P = 0.288$ ) or site ( $P = 0.137$ ) (Table 3).

## DISCUSSION

In this study, the partial DNA sequence for photolyase was identified in three species of sea urchin, including the Antarctic species *S. neumayeri*. Using this sequence, photolyase expression in the developmental stages of *S. neumayeri*, and in its embryos in response to *in situ* exposure ambient light was examined.

#### Photolyase DNA sequences

Photolyase enzymes are monomeric proteins made up of 454–614 amino acids, which contain a noncovalently bound FAD (13–15). There are varying degrees of similarity amongst the photolyase sequences available, ranging from 15% to 70%. The area that appears to exhibit the greatest similarity between the classes is the 150 amino acids at the C-terminus. These areas are known to be the FAD binding site, confirmed by mutagenesis, protein chemistry and crystallography (12,18). A 300 bp sequence, first identified in *S. purpuratus*, amplified in the three species of sea urchins examined in this study (*S. neumayeri*, *E. chloroticus* and *S. franciscanus*). This sequence is highly conserved not only among the sea urchin species, but also between distantly related taxa, and corresponds to the FAD binding site (12).

Photolyase also typically contains a second noncovalently bound chromophore (most often 5, 10-methyltetrahydrofolate), and it is probable that photolyase has a second highly conserved binding region. An alignment of two distantly related species, *G. gallus* and *Drosophila melanogaster*, failed to reveal another region as conserved as the one associated with the FAD binding site; however, a region near the 5'-end was identified that was conserved enough for primer design. Using a primer designed from this region, in conjunction with a primer that annealed within the part of the sequence which codes for the FAD binding site, it was possible to amplify a 1200 bp sequence from *S. franciscanus* which may correspond with the light-harvesting cofactor binding site (NCBI accession reference: FJ812411).

Previous work on sea urchin embryos (19) and other Antarctic zooplankton (7) has indicated that photoreactivation is slower than in temperate and tropical counterparts, which would suggest a lack of cold adaptation in photolyase. Temperature compensation in enzymes can involve structural changes associated with amino acid substitutions (23),

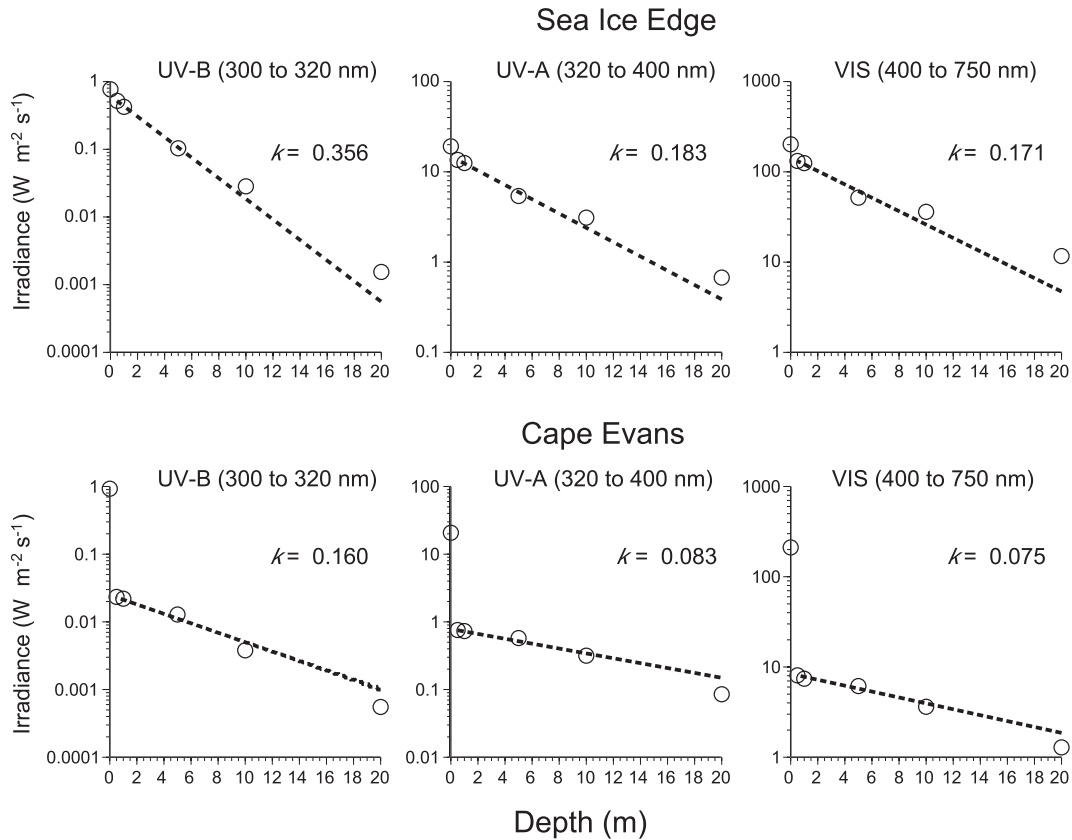


**Figure 4.** UV-B (300–320 nm), UV-A (320–400 nm) and PAR (400–750 nm) irradiances ( $\text{W m}^{-2}$ ) at the sea surface and with depth for Cape Evans (31 October 2007) and the sea ice edge (1 November 2007) in McMurdo Sound. Lines fitted to data are  $I_D = I_0 \times e^{-kd}$ , where  $I_D$  is irradiance at depth  $d$ ,  $I_0$  is irradiance at depth 0.5 m and  $k$  is the attenuation coefficient.

although our limited sequences do not allow us to comment on structural differences (or lack of) in photolyases among the Antarctic and temperate sea urchins. In addition, our sequences belong to the highly conserved FAD binding site, a region unlikely to show structural changes.

#### Photolyase expression during *Sterechinus* early development

We did not quantify the relative levels of photolyase mRNA in the gonad and larvae of *Sterechinus*, but using PCR we established its presence in the gonad and all larval stages examined. This confirms previous observations that photo-reactivation occurs in blastula, gastrula and the pluteus stages of sea urchin larvae and embryos (19). Photolyase mRNA was also found in the ovaries of all four sea urchin species (*S. franciscanus*, *S. purpuratus*, *E. chloroticus* and *S. neumayeri*) examined. Expression of photolyase in ovaries and unfertilized eggs has also been reported for *D. melanogaster* (24) and *Engraulis mordax* (25), respectively, and its existence in tissue located within the dark adult body cavity is an interesting finding given the protein requires light to carry out catalysis. There are two possible explanations for this; either photolyase serves some other function yet to be identified, or photolyase is being expressed in ovaries and eggs before spawning. Photolyase mRNA concentrations in *D. melanogaster* ovaries were found to be higher than in eggs and embryos (24). This was suggested to be a maternal effect, where oocytes were being endowed with photolyase mRNA from the parent (24).

Transferring photolyase mRNA to prespawning ovaries could prove beneficial, as the resulting photolyase in eggs and embryos would mitigate the deleterious effects of UV-R immediately upon spawning and prevent any delay in photolyase production that might result in DNA dimer accumulation.

While our results show the constitutive expression of photolyase in all developmental stages, the amount of the enzyme initially endowed may be insufficient to repair elevated levels of DNA damage. For example, previous work on photoreactivation in sea urchin embryos showed a 1 h delay before repair of CPDs was measurable (19). This result suggested that photolyase was not initially present in high enough concentrations to repair the damage that was induced by the UV-R in an *in vitro* setting. The upregulation of photolyase expression observed *in situ* and in response to higher UV-R exposure also suggests that while photolyase is expressed constitutively, an increase in its production is required to repair the amounts of DNA damage that can occur naturally.

#### *In situ* photolyase expression in response to UV-R

In terms of photolyase expression, the response of organisms to UV-R exposure and resulting DNA damage is species specific. Whereas photolyase is often constitutively expressed independent of UV-R exposure (25–27), expression of photolyase in *Rana sylvatica* embryos has been positively correlated with UVB dose (27), and in *Carassius auratus*, by

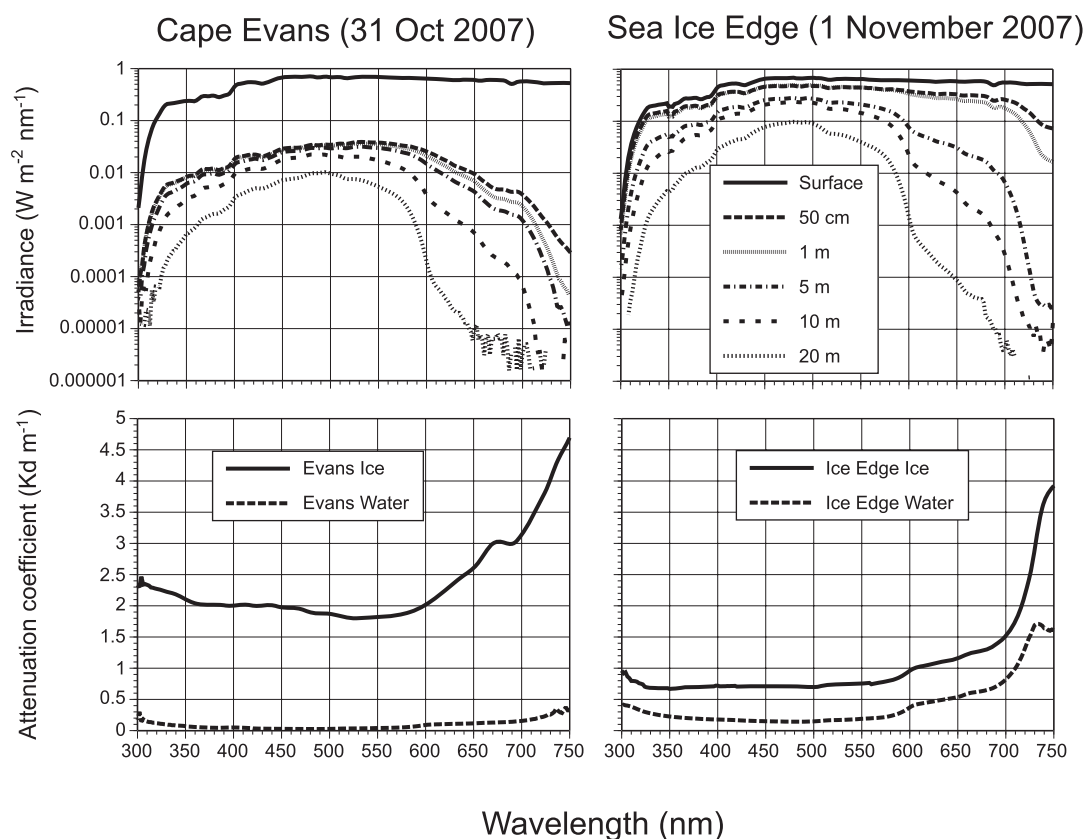


**Figure 5.** Spectral irradiances versus wavelength (300–750 nm) for Cape Evans and the sea ice edge, McMurdo Sound. Bulk attenuation coefficients ( $K_d \text{ m}^{-1}$ ) versus wavelengths between 300 and 750 nm through the sea ice (sea ice surface to 0.5 m below the sea ice) and through the water column (1–5 m depth) are indicated.

**Table 1.** Average daily UV-R dose (290–400 nm) estimated for Cape Evans and the sea ice edge.

Depth (m)	Average daily UV-R dose ( $\text{kJ m}^{-2} \text{ day}^{-1}$ )	
	Cape Evans*	Sea ice edge†
0.5	105.49	
1	82.69	
5	51.33	1266.48
10	23.74	288.57

\*31 October to 7 November 2007. †1 November to 10 November 2007.

exposure to visible light (26). The present study suggests that while there is also constitutive photolyase expression in *Sterechinus* embryos, expression does vary with depth and UV-R dose. Expression was highest in the embryos that received an average daily dose of UV-R of  $105.4 \text{ kJ m}^{-2} \text{ day}^{-1}$ , and decreased with reduced UV-R exposure. Under the Cape Evans sea ice, photolyase mRNA was higher in the UV-T treatment than in the UV-O treatment except for samples from 2.0 m, and was also higher in the UV-O treatments at 0.5 and 2.0 m than it was at 5.0 and 10.0 m. These results suggest that photolyase expression is induced in sea urchin embryos by two possible mechanisms. The first is that induction is a product of exposure to UV-R or resulting CPD concentration. In this respect, an unidentified long-wave UV-B-specific receptor has recently been shown to mediate the transcription of photolyase

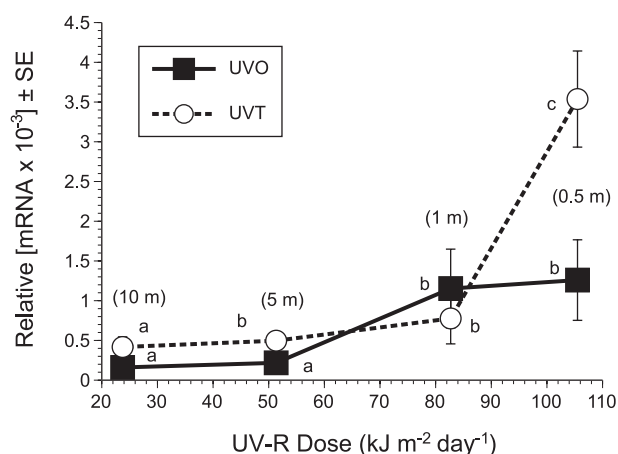


**Figure 6.** Average ( $\pm$  SE) expression of photolyase (normalized to actin) in blastula stage larvae of *Sterechinus neumayeri* as a function of daily UV-R dose at Cape Evans (31 October to 7 November 2007). Embryos were either exposed to full spectrum ambient light (UV-T), or visible light only with UV-R blocked (UV-O). The depth of each exposure is given in parentheses. Exposures were for 7 days. Significant differences ( $P < 0.05$ ) among treatments were tested using a Tukey's *post hoc* test, and are indicated on the figure (treatments sharing the same letter were not significantly different).  $N = 3$  for each column.

in the plants (28), and the existence of a comparable system in sea urchin embryos would be consistent with the lower expression of photolyase we observed when UV-B is removed.

**Table 2.** Two-way ANOVA of the photolyase expression ([mRNA] normalized to actin) in the blastula of *Sterechninus neumayeri* treated at four depths (0.5, 1, 5 and 10 m) with either full spectrum light or full spectrum light with UV-R blocked. Concentrations are  $\ln(x + 1)$  transformed.

Source	SS	d.f.	MS	F-ratio	P
Analysis of variance					
Model	7	3.379	0.482	4.166	0.008
Error	16	1.854	0.115		
Total	23	5.233			
Source	SS	d.f.	F-ratio	P	
Test of effects					
Depth	3	2.612	7.516	0.002	
Light treatment	1	0.511	4.415	0.051	
Depth $\times$ light	3	0.585	1.683	0.210	

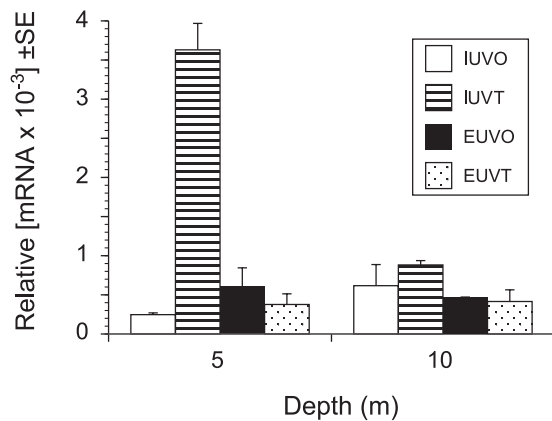


**Figure 7.** Expression of photolyase ([mRNA] normalized to actin) in *Sterechninus neumayeri* blastula from UV-O and UV-T treatments at 5 and 10 m depth at Cape Evans (31 October to 7 November 2007) and the sea ice edge, McMurdo Sound (1 November to 10 November 2007). The treatment are: IUVO = sea ice edge no UV; IUVT = sea ice edge full UV; EUVO = Cape Evans no UV; EUVT = Cape Evans full UV.

**Table 3.** Three-way ANOVA of the photolyase expression ([mRNA] normalized to actin) in the blastula of *Sterechninus neumayeri* treated at two depths (5 and 10 m) at Cape Evans and the sea ice edge, with either full spectrum light or full spectrum light with UV-R blocked. Concentrations are  $\ln(x + 1)$  transformed.

Source	SS	d.f.	MS	F-ratio	P
Analysis of variance					
Model	0.000011	3	0.0000037	1.934	0.156
Error	0.000038	20	0.0000019		
Total	0.000049	23			
Source	SS	d.f.	F-ratio	P	
Test of effects					
Site	0.0000046	1	2.403	0.137	
Light treatment	0.0000042	1	2.207	0.153	
Depth	0.0000023	1	1.194	0.288	

Secondly, as expression of photolyase decreased with depth in the UV-O treatment, it appears that exposure to higher visible light can induce photolyase expression, albeit at a slower rate. Indeed, previous work has shown that visible light is used as a proxy for UV-R exposure in *C. auratus* and can induce expression of photolyase (26).

Ultraviolet radiation has been shown to penetrate sea ice and have a detrimental effect on larvae (3). Without sea ice, the level of UV-R penetrating the water column would significantly increase; so to determine how a reduction in sea ice might effect embryos in terms of photolyase expression, two identical *in situ* experiments under sea ice (Cape Evans) and open water (sea ice edge) were compared. The dose of UV-R at 5 and 10 m depths was significantly greater at the sea ice edge, 1261 and 287.7  $\text{kJ m}^{-2} \text{day}^{-1}$ , than at Cape Evans, 51.32 and 23.6  $\text{kJ m}^{-2} \text{day}^{-1}$ . Photolyase mRNA was higher in the UV-T treatment at the ice edge that received 1261  $\text{kJ m}^{-2} \text{day}^{-1}$  when compared with all the other samples, but not to a statistically significant level. While the current experiments were not conclusive, the higher mRNA concentrations observed in the open water conditions are certainly indicative of the elevated levels of photolyase expression that would be expected under conditions of thinning or reduced sea ice.

## CONCLUSIONS

These data show that although photolyase is constitutively expressed, exposure to UV-R can induce expression of photolyase in *S. neumayeri* embryos. This is consistent with previous findings that UV-R could damage the DNA of embryos *in situ* (3,6,8). Higher rates of expression in response to higher UV-R exposure (*i.e.* with both decreased depth and sea ice coverage) indicate that future climate change scenarios that increase light in the Antarctic marine environment (*i.e.* reduced sea ice coverage, [29] are likely to induce higher levels of DNA damage and the upregulation of photolyase expression. This would represent a metabolic cost to Antarctic sea urchin embryos, which, given their slow metabolism (30), could represent a significant physiological cost. Although this may not increase mortality directly, it may reduce development rates that are already very slow in Antarctic species (*i.e.* 114 days to complete development in *Sterechninus*, 21). Planktonic larval stages experience very high mortality rates (*i.e.*  $\approx 16\% \text{day}^{-1}$ ) (31), and so any delay in development rates is likely to lead to lower recruitment rates and a reduction in population viability over the long term.

*Acknowledgements*—We especially thank Antarctica New Zealand for their logistical support over two field seasons. Thanks to Professor Michael Lesser and Dr. Adam Marsh for discussions and suggestions during the research. We also thank staff at the Portobello Marine Laboratory and the Department of Biochemistry, University of Otago, for assistance with our research. This research was generously funded by a University of Otago Research Grant (M.D.L., M.F.B. and C.J.M.).

## REFERENCES

- Pakulski, J. D., J. P. Kase, J. A. Meador and W. H. Jeffrey (2008) Effect of stratospheric ozone depletion and enhanced ultraviolet radiation on marine bacteria at Palmer Station, Antarctica in the early austral spring. *Photochem. Photobiol.* **84**, 215–221.

2. Smith, R. C., B. B. Prézelin, K. S. Baker, R. R. Bidigare, N. P. Boucher, T. Coley, D. Karentz, S. MacIntyre, H. A. Matlick, D. Menzies, M. Ondrusek, Z. Wan and K. J. Waters (1992) Ozone depletion: Ultraviolet radiation and phytoplankton biology in Antarctic waters. *Science* **255**, 952–959.
3. Lesser, M. P., M. D. Lamare and M. F. Barker (2004) Transmission of ultraviolet radiation through the Antarctic annual sea ice and its biological effects on sea urchin embryos. *Limnol. Oceanogr.* **49**(6), 1957–1963.
4. Karentz, D. (1994) Ultraviolet tolerance mechanisms in Antarctic marine organisms. In *Ultraviolet Radiation in Antarctica: Measurements and Biological Effects* (Edited by C. S. Weiler and P. A. Penhale), *Antarct. Res. Ser.* **62**, 93–110. American Geophysical Union, Washington, DC.
5. Karentz, D. (1991) Ecological considerations of Antarctic ozone depletion. *Antarct. Sci.* **3**, 3–11.
6. Lamare, M. D., M. F. Barker and M. P. Lesser (2007) *In situ* rates of DNA damage and abnormal development in Antarctic and non-Antarctic sea urchin embryos. *Aquatic Biology* **1**, 21–32.
7. Malloy, K. D., M. A. Holman, D. Mitchell and H. W. Detrich (1997) Solar UVB-induced DNA damage and photoenzymatic DNA repair in Antarctic zooplankton. *Proc. Natl Acad. Sci. USA* **94**(4), 1258–1263.
8. Karentz, D. and I. Bosch (2001) Influence of ozone-related increases in ultraviolet radiation on Antarctic marine organisms. *Am. Zool.* **41**, 3–16.
9. Karentz, D., I. Bosch and D. M. Mitchell (2004) Limited effects of Antarctic ozone depletion on sea urchin development. *Mar. Biol.* **145**, 277–292.
10. Sinha, R. P. and D.-P. Häder (2002) UV-induced DNA damage and repair: A review. *Photochem. Photobiol. Sci.* **1**, 225–236.
11. Cadet, J., T. Douki, D. Gasparutto and J.-L. Ravanat (2003) Oxidative damage to DNA: Formation, measurement and biochemical features. *Mutat. Res.* **531**, 5–23.
12. Sancar, A. (2003) Structure and function of DNA photolyase and cryptochrome blue-light photoreceptors. *Chem. Rev.* **103**, 2203–2237.
13. Aubert, C., M. H. Vos, P. Mathis, A. P. M. Eker and K. Brettel (2000) Intraprotein radical transfer during photoactivation of DNA photolyase. *Nature* **405**, 586–590.
14. Weber, S. (2005) Light-driven enzymatic catalysis of DNA repair: A review of recent biophysical studies on photolyase. *Biochim. Biophys. Acta* **1707**, 1–23.
15. Essen, L. O. and T. Klar (2006) Light-driven DNA repair by photolyases. *Cell. Mol. Life Sci.* **63**, 1266–1277.
16. Fujihashi, M., N. Numoto, Y. Kobayashi, A. Mizushima, M. Tsujimura, A. Nakamura, Y. Kawarabayashi and K. Miki (2007) Crystal structure of archaeal photolyase from *Sulfolobus tokodaii* with two FAD molecules: Implication of a novel light-harvesting cofactor. *J. Mol. Biol.* **365**, 903–910.
17. Medvedev, D. and A. A. Stuchebrukhov (2001) DNA repair mechanism by photolyase: Electron transfer path from the photolyase catalytic FADH<sup>-</sup> to DNA thymine dimer. *J. Theor. Biol.* **210**, 237–248.
18. Takumi, U., A. Kato, Y. Ogawa, T. Torizawa, S. Kuramitsu, S. Iwai, H. Terasawa and I. Shimada (2004) NMR study of repair mechanism of DNA photolyase by FAD-induced paramagnetic relaxation enhancement. *J. Biol. Chem.* **279**(50), 52574–52579.
19. Lamare, M. D., M. F. Barker, M. P. Lesser and C. J. Marshall (2006) DNA photorepair in echinoid embryos: Effects of temperature on repair rate in Antarctic and non-Antarctic species. *J. Exp. Biol.* **209**(24), 5017–5028.
20. Bosch, I., K. A. Beauchamp, E. Steele and J. S. Pearse (1987) Development, metamorphosis, and seasonal abundance of embryos and larvae of the Antarctic sea urchin *Sterechinus neumayeri*. *Biol. Bull.* **173**, 126–135.
21. Shilling, F. M. and D. T. Manahan (1994) Early metabolism and amino acid transport during early development of Antarctic and temperate echinoderms. *Biol. Bull.* **187**, 398–407.
22. Chomczynski, P. and N. Sacchi (1987) Single-step method of RNA isolation by acid guanidinium thiocyanate-phenol-chloroform extraction. *Anal. Biochem.* **162**, 156–159.
23. Somero, G. N. (1995) Proteins and temperature. *Annu. Rev. Physiol.* **57**, 43–68.
24. Todo, T., H. Ryo, H. Takemori, H. Toh, T. Nomura and S. Kondo (1994) High-level expression of the photorepair gene in *Drosophila* ovary and its evolutionary implications. *Mutat. Res.* **315**, 213–228.
25. Vetter, R. D., A. Kurtzman and T. Mori (1999) Diel cycles of DNA damage and repair in eggs and larvae of Northern Anchovy, *Engraulis mordax*, exposed to solar ultraviolet radiation. *Photochem. Photobiol.* **69**(1), 27–33.
26. Yasuhira, S. and A. Yasui (1992) Visible light-inducible photolyase gene from the goldfish *Carassius auratus*. *J. Biol. Chem.* **267**(36), 25644–25647.
27. Smith, M. A., C. M. Kapron and M. Berrill (2000) Induction of photolyase activity in wood frog (*Rana sylvatica*) embryos. *Photochem. Photobiol.* **72**(4), 575–578.
28. Ioki, M., S. Takahashi, N. Nakajima, K. Fujikura, M. Tamaoki, H. Saji, A. Kubo, M. Aono, M. Kanna, D. Ogawa, J. Fukazawa, Y. Oda, S. Yoshida, M. Watanabe, S. Hasezawa and N. Kondo (2008) An unidentified ultraviolet-B-specific photoreceptor mediates transcriptional activation of the cyclobutane pyrimidine dimer photolyase gene in plants. *Planta* **229**, 25–36.
29. Newman, P. A., E. R. Nash, S. R. Kawa, S. A. Montzka and S. M. Schauffer (2006) When will the Antarctic ozone hole recover? *Geophys. Res. Lett.* **33**, L12814.
30. Hoegh-Guldberg, O. H., J. R. Welborn and D. T. Manahan (1991) Metabolic requirements of Antarctic and temperate asteroid larvae. *Antarct. J.* **26**, 163–165.
31. Lamare, M. D. and M. F. Barker (1999) *In situ* estimates of larval development and mortality in the New Zealand sea urchin *Evechinus chloroticus* (Echinodermata: Echinoidea). *Mar. Ecol. Prog. Ser.* **180**, 197–211.